

## Stable Equidistant Step Trains during Crystallization of Insulin

Olga Gliko, Ilya Reviakine, and Peter G. Vekilov

*Department of Chemical Engineering, University of Houston, Houston, Texas 77204, USA*

(Received 15 February 2003; published 6 June 2003)

Bunching of growth steps plagues layerwise crystallization of materials in laboratory, industrial, and geological environments, and theory predicts that equidistant step trains are unstable under a variety of conditions. Searching for an example of stable equidistant step trains, we monitored the generation and spatiotemporal evolution of step trains on length scales from 100 nm to 1 mm during the crystallization of insulin, using atomic force microscopy and phase-shifting interferometry. We show that near-equidistant step trains are generated by single and cooperating screw dislocation. The lack of step-step interaction and the overall transport-controlled growth regime further regularize the step train and ensure the stability of the obtained equidistant arrangement.

DOI: 10.1103/PhysRevLett.90.225503

PACS numbers: 81.10.Aj, 47.20.Bp, 68.35.Ct, 87.90.+y

During growth of crystalline materials by the spreading of layers, equidistant step trains often lose stability and break into bunches of steps interspersed with bands of low step density [1]. In the resulting material, the step bunches leave trails of higher defect density and, in this way, lower its quality and utility [2]. On the other hand, it has recently been suggested that the capability to control step bunching could be utilized for the generation of step patterns for use as nanostructure templates [3].

Several microscopic factors for the loss of step train stability and step bunch formation have been considered: (i) step-step interactions due to competition for supply via surface diffusion [4,5], (ii) interactions due to overlapping elastic fields of the steps [6], (iii) asymmetry for incorporation from top and lower terraces [4,7], (iv) asymmetry due to solution flow [8] or electric current [9], and (v) impurity effects [10].

The step bunching instability in solution crystallization can also be addressed from the viewpoint of macroscopic kinetics, with the equidistant step train viewed as the steady state and the bunches representing the kinetic fluctuations occurring after stability loss [11]. Within this model, a process comprising two coupled stages, such as transport through the solution and incorporation into the steps, is unstable provided that one of the stages follows a nonlinear kinetic law. The factors considered in the microscopic approaches have been viewed among the sources of nonlinearity of the second stage of the macroscopic formalism—incorporation into steps [12].

An investigation of the step bunching instability during the crystallization of the protein lysozyme revealed a strong step-step interaction through overlapping surface diffusion supply fields, which provides for heavy step bunching under a broad range of experimental conditions [13,14]. A similar investigation with ferritin revealed step bunches, which are generated due to the strongly nonlinear two-dimensional nucleation of new layers. Since the individual steps do not interact, the step bunches decay as they move along their pathway [15,16]. With

both proteins, it was shown that overlapping of the bulk solution supply fields of the steps only provides for a weak interaction that does not induce step bunching [16,17], and that changing the experimental conditions to regimes where the control of the kinetics is shifted either to the transport or to the incorporation stage reduces step bunching [14–16,18]. The results with ferritin suggest that, in systems with weakly or noninteracting steps controlled by transport, the stable growth mode is that via equidistant step trains [15,16]. However, with ferritin this stable regime is not realized: Step bunches are produced because of the nonlinear step generation and cannot dissipate over the relatively short ( $\sim 0.5$  mm) step pathways.

The objective of this Letter is to demonstrate that equidistant step trains are stable and constitute the dominant growth mode in systems where the steps (i) propagate without interaction and (ii) are generated by a linear kinetic process. We found that the crystallization of the protein insulin, which underlies the production of several diabetes medications [19], is such a system. In addition, we found that further stabilization of the equidistant step trains is provided by the transport control of the growth process.

Rhombohedral ( $R3$ ) crystals of porcine insulin grew on 12-mm Teflon-coated metal disks [20] from solutions containing up to  $1 \text{ mg ml}^{-1}$  insulin,  $0.05M$  sodium citrate,  $0.005M$   $\text{ZnCl}_2$ , 0% and 15% (v/v) acetone,  $0.001M$  HCl, at  $pH = 7.0$  and temperature  $T = 27^\circ\text{C}$  [21]. The solution supersaturation was calculated as  $(C - C_e)C_e^{-1}$ , where  $C$  is insulin concentration and the solubility at  $T = 27^\circ\text{C}$  is  $C_e = 0.15 \text{ mg ml}^{-1}$  at zero acetone concentration, and  $C_e = 0.35 \text{ mg ml}^{-1}$  at 15% acetone (Bergeron *et al.*, unpublished results). Images of the crystal surface were collected *in situ* during growth using atomic force microscopy (AFM) in tapping mode [22]. The scanning and tapping parameters were adjusted so that continuous imaging did not affect the morphology of the imaged part of the surface, or the rate of the monitored processes. This

was verified by varying the scan sizes and the time intervals between scans. For details on similar observations with apoferritin, see [23].

Growth of  $\{100\}$  (or  $\{10\bar{1}1\}$ ) insulin crystal faces proceeds by spreading of layers, which are typically generated by screw dislocations. In some instances, on crystals consisting of several blocks, new layers were generated by two-dimensional (2D) nucleation at the block boundaries. 2D nucleation was likely facilitated at these locations by the lattice misfit in a direction perpendicular to the monitored face [24]. Figure 1(a) shows a single screw dislocation producing a four-sided polygonal spiral, in which the straight segments are parallel to the respective crystal edges. The sides of resulting hillock are not related by any of the symmetry elements belonging to the  $R3$  crystallographic group of the crystal. The dislocation source in Fig. 1(b) features both left- and right-handed screw dislocations. In all studied cases ( $\sim 40$ ), single and multiple dislocation sources produced near-equidistant step trains. As with other systems [25], the density of the steps generated by single dislocations followed a weaker than linear increase with insulin concentration, in accordance with theoretical expectations of a  $\sim \ln C$  law [25,26]. The density of the steps generated by multiple dislocations was not an apparent function of the insulin concentration, similar to Ref. [27].

Figures 2(a)–2(c) illustrate the high stability of the equidistant step trains—they were preserved at all locations on the crystal surface, near and far (at  $\sim 300 \mu\text{m}$ ) from the dislocation source, and in a wide range of supersaturations. Figure 2(a) shows that, in contrast to previous observations with other systems [28], the equidistant step trains remain stable even as the steps pass over obstacles, such as dislocation outcrops.

To explore if any of the microscopic factors (i)–(v) above affect the kinetics of the individual growth steps, we monitored the spatiotemporal evolution of a step train generated by irregular 2D nucleation on a grain boundary and exhibiting variable step density. We disabled the slow scanning axis of AFM (for details and tests of this imag-

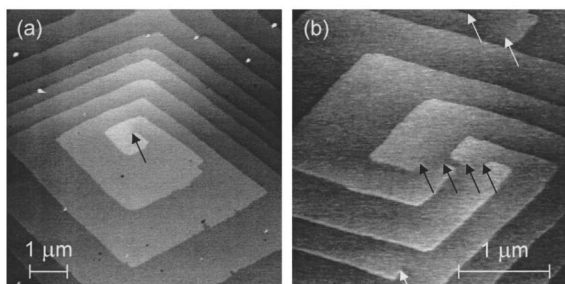


FIG. 1. Generation of new layers by screw dislocations. (a) Single dislocation produces hillock. (b) Four dislocations, indicated with black arrows, work in cooperation to produce a hillock, with three dislocations, indicated with white arrows, on hillock side.

ing mode, see [16,19]). Figure 2(d) shows a pseudoimage obtained in this mode, in which the vertical axis represents time. The slope of a step trace is reciprocal to the step velocity, and the local step density is determined from the distances between the step traces at a given time. The data in Fig. 2(d) reveal that closely spaced steps move with the same velocity as widely spaced ones, and that steps preceded by a closely positioned neighbor move with the same velocity as steps closely followed by another step. The first observation indicates that the steps do not compete for supply from the surface, that elastic interactions or impurity effects do not slow down or accelerate the steps, and that competition for supply from the solution bulk does not affect the step motion. The second observation indicates that, correspondingly, there is now asymmetry in the incorporation into a step from its top and lower terraces. The high stability of the equidistant step trains is illustrated by the fluctuations in interstep distances in Fig. 2(d), likely due to surface supersaturation fluctuations—in contrast to lysozyme [14], they do not trigger a cascade of step bunches.

For insight into the step dynamics over longer times and distances, we applied phase-shifting interferometry [30]. While inferior in spatial resolution to AFM, interferometry is nonintrusive and allows *in situ* monitoring of

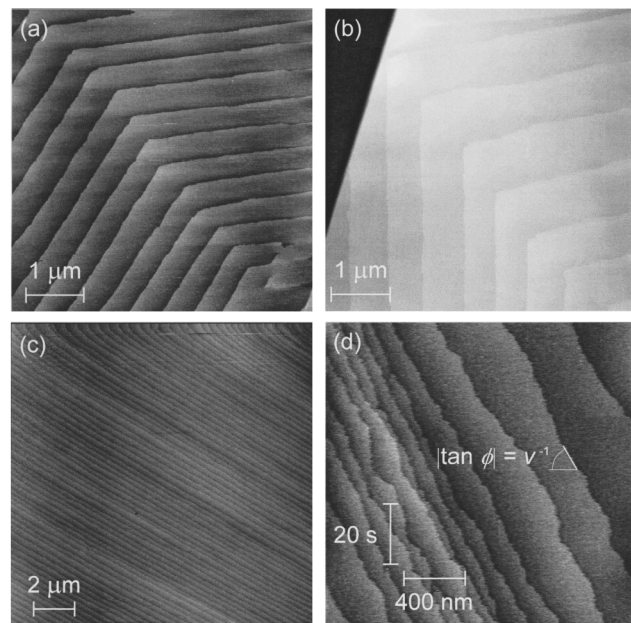


FIG. 2. Step trains on the surface of insulin crystals. (a)–(c) Equidistant step trains (a) after passing over a dislocation outcrop,  $(C - C_e)C_e^{-1} = 0.8$ , (b) near a grain boundary,  $(C - C_e)C_e^{-1} = 0.8$ , (c) far from the dislocation group, which produces the monitored step train,  $(C - C_e)C_e^{-1} = 3.5$ . (d) Spatiotemporal evolution of step train at  $(C - C_e)C_e^{-1} = 2.5$ . A pseudoimage recorded by disabling the slow scan axis so that the vertical axis represents time. Time increases from top to bottom; steps move from left to right. The slope of the step trace equals the reciprocal step velocity  $v^{-1}$ .

the kinetics and microscopic morphologies across entire macroscopic facets. The phase-shifting algorithm employs five-image sequences captured within 1 s and processed to reconstruct the surface morphology with a depth resolution of 5 nm across a field of view of  $1 \times 1 \text{ mm}^2$  (for further details, see [15,30]). Time traces of growth rate and local slope, proportional to step density, are recorded at selected locations on the crystal surface with time resolution 1 s. Figure 3(a) shows a phase-wrapped image representing the morphology of an insulin crystal face with size  $230 \mu\text{m}$  at supersaturation  $(C - C_e)C_e^{-1} = 0.3$ . Two major dislocation hillocks are seen near the right top part of the surface. Figures 3(b) and 3(c) show time traces of growth rate and local slope recorded at a location far from the dislocation source shown in Fig. 3(a). Figures 3(b) and 3(c) show that growth kinetics are steady, and step density only undergoes minor fluctuations.

The spatial characteristics of step patterns are revealed by the height profiles in Fig. 4(a), taken along the direction of step propagation around the location far from the layer source shown in Fig. 3(a). Subtracting average surface slope, we obtain the differential profile shown in Fig. 4(b). It shows no step bunches, in agreement with the steady kinetics revealed by corresponding time traces in Figs. 3(b) and 3(c). Thus, the interferometry characterization supports the conclusion that the growth

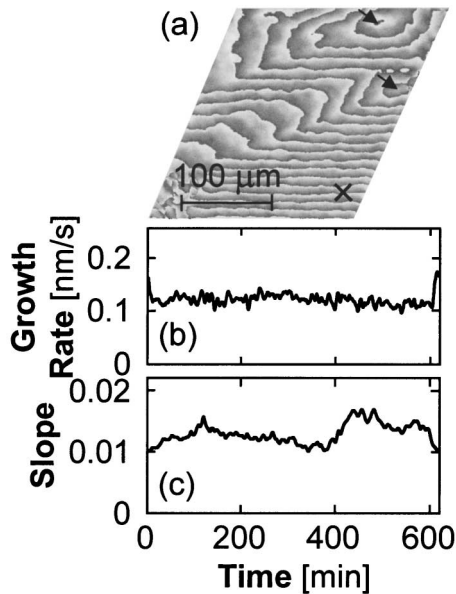


FIG. 3. Interferometric characterization of the surface morphology and its evolution during growth at  $(C - C_e)C_e^{-1} = 0.3$ . (a) Phase-wrapped interferograms. Lighter color codes for greater height; the discontinuities in gray scale correspond to height difference of  $0.12 \mu\text{m}$ . (b),(c) Time traces of normal growth rate in (b) and local slope in (c), recorded at location, indicated by  $\times$  in (a), far from step sources, indicated with arrows.

of insulin crystals is stable and proceeds via equidistant step trains.

To explain the stability of step trains against the small fluctuations evidenced by AFM and interferometry data, we evaluate the kinetic Peclet number  $Pe_k = \beta p \delta / D$ , where  $\beta$  is the step kinetic coefficient of the insulin,  $p$  is slope,  $\delta$  is the characteristic diffusion layer thickness, and  $D$  is insulin diffusivity. Using  $\beta = 6 \times 10^{-3} \text{ cm s}^{-1}$  (Reviakine *et al.*, unpublished),  $p = 1.2 \times 10^{-2}$  from, e.g., Fig. 3(c),  $D = 8 \times 10^{-7} \text{ cm}^2 \text{ s}^{-1}$  [31], and choosing  $\delta \sim 2 \times 10^{-2} \text{ cm}$  (a low estimate, stemming from a direct determination and an evaluation in simulations of the convective-diffusive transport [32]), we get  $Pe_k \approx 1.7$ . Since  $Pe_k$  is the ratio of the characteristic rates of surface kinetics  $\beta p$  to that of transport in the solution  $D/\delta$ ,  $Pe_k > 1$  is viewed as an indication of transport-controlled growth [12,33].

In a transport-controlled regime, a fluctuation of, say, higher step density would dissipate. Indeed, areas of high density of noninteracting steps are also areas of local growth rate maxima and, in a transport-controlled regime, supersaturation minima. As another consequence of the transport-controlled regime, the solute diffusion field near the interface lags behind the step pattern that generates it. Thus, a step train segment of high step density moves into an area of higher supersaturation, while the trailing segments of lower step density find themselves in an area of lower supersaturation. The steps trailing behind the step bunch are prevented from catching up with the bunch and increasing its height. A self-consistent analytical solution has shown that this results in dissipating step bunches and stabilization of the equidistant step trains [34].

From the general perspective of the macroscopic kinetics viewpoint, insulin crystallization is an example in which the lack of sources of nonlinearity in the surface

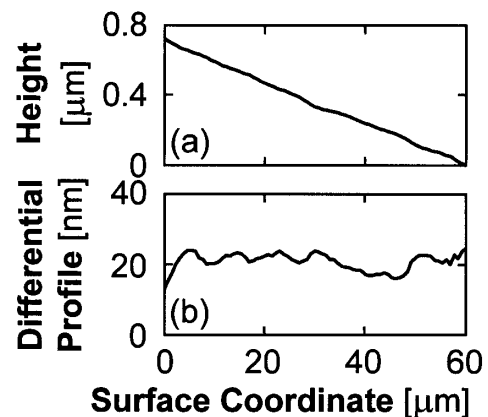


FIG. 4. Quantification of surface morphology by phase-shifting interferometry around the locations far from dislocation source shown in Fig. 3(a). (a) Height profiles along direction of step propagation. (b) Corresponding differential profiles obtained by subtraction of average surface slope.

kinetics (unsteady layer generation, or step-step interactions), combined with having only one of the two coupled processes control the overall rate of growth, provides for a stable steady state of the growth kinetics, i.e., equidistant step train.

In the terms of the microscopic stability models, the results discussed in this Letter, in the context of the previous results with lysozyme and ferritin, show that if (i) growth steps are generated by a process the rate of which is a linear or weaker function of the local supersaturation, (ii) during their motion they do not interact, and (iii) transport of material from the solution is slower than incorporation at the steps, then no step bunching instability evolves and equidistant step trains are the stable kinetic state of the surface.

We thank L. Bergeron and L. Filobello for insulin solubility data and crystallization conditions, and A. A. Chernov for helpful suggestions. This work was supported by the Office of Physical and Biological Research, NASA, through Grants No. NAG8-1854 and No. NAG8-1824.

- 
- [1] I. Sunagawa and P. Bennema, *J. Cryst. Growth* **46**, 451 (1979); E. D. Williams and N. C. Bartelt, *Science* **251**, 393 (1991).
- [2] E. Bauser, in *Handbook of Crystal Growth*, edited by D. T. J. Hurle (North-Holland, Amsterdam, 1994), Vol. 3b, p. 879; J. J. De Yoreo, N. P. Zaitseva, J. D. Lee, T. A. Land, I. Smolski, and E. B. Rudneva, *J. Cryst. Growth* **169**, 741 (1996); P. G. Vekilov and F. Rosenberger, *Phys. Rev. E* **57**, 6979 (1998).
- [3] R. M. Tromp, R. M. Ross, and M. C. Reuter, *Phys. Rev. Lett.* **84**, 4641 (2000); M. Sato, M. Uwaha, and Y. Saito, *Phys. Rev. B* **62**, 8452 (2000); A. Pimpinelli, V. Tonchev, A. Videcoq, and M. Vladimirova, *Phys. Rev. Lett.* **88**, 206103 (2002).
- [4] M. Sato and M. Uwaha, *Phys. Rev. B* **51**, 11 172 (1995).
- [5] M. Uwaha, Y. Saito, and M. Sato, *J. Cryst. Growth* **146**, 164 (1995).
- [6] G. S. Bales and A. Zangwill, *Phys. Rev. B* **41**, 5500 (1990).
- [7] R. L. Schwoebel and E. J. Shipsey, *J. Appl. Phys.* **37**, 3682 (1966).
- [8] A. A. Chernov, *J. Cryst. Growth* **118**, 333 (1992); S. R. Coriell, B. T. Murray, A. A. Chernov, and G. B. McFadden, *J. Cryst. Growth* **169**, 773 (1996).
- [9] S. Stoyanov and V. Tonchev, *Phys. Rev. B* **58**, 1590 (1998).
- [10] F. C. Frank, in *Growth and Perfection of Crystals*, edited by R. H. Doremus, B. W. Roberts, and D. Turnbull (Wiley, New York, 1958), p. 411; J. P. Van der Eerden and H. Mueller-Krumbhaar, *Phys. Rev. Lett.* **57**, 2431 (1986); S. Y. Potapenko, *J. Cryst. Growth* **147**, 223 (1995).
- [11] P. Gray and S. K. Scott, *Chemical Oscillation and Instabilities. Nonlinear Chemical Kinetics* (Clarendon, Oxford, 1990); P. J. Ortoleva, *Geochemical Self-Organization* (University Press, Oxford, 1994); R. M. Noyes and R. J. Fields, *Ann. Rev. Phys. Chem.* **25**, 95 (1974); M. C. Cross and P. C. Hohenberg, *Rev. Mod. Phys.* **65**, 851 (1993).
- [12] P. G. Vekilov and J. I. D. Alexander, *Chem. Rev.* **100**, 2061 (2000).
- [13] P. G. Vekilov, J. I. D. Alexander, and F. Rosenberger, *Phys. Rev. E* **54**, 6650 (1996).
- [14] P. G. Vekilov, H. Lin, and F. Rosenberger, *Phys. Rev. E* **55**, 3202 (1997).
- [15] O. Gliko and P. G. Vekilov, *J. Phys. Chem.* **106**, 11800 (2002).
- [16] H. Lin, S.-T. Yau, and P. G. Vekilov, *Phys. Rev. E* **67**, 031606 (2003).
- [17] F. Rosenberger, H. Lin, and P. G. Vekilov, *Phys. Rev. E* **59**, 3155 (1999).
- [18] P. G. Vekilov and F. Rosenberger, *Phys. Rev. Lett.* **80**, 2654 (1998).
- [19] J. Brange, *Galenics of Insulin* (Springer-Verlag, Berlin, 1987).
- [20] D. J. Müller, M. Amrein, and A. Engel, *J. Struct. Biol.* **119**, 172 (1997).
- [21] M. M. Harding, D. C. Hodgkin, A. F. Kennedy, A. O'Connor, and P. D. J. Weitzmann, *J. Mol. Biol.* **16**, 212 (1966).
- [22] P. K. Hansma, J. P. Cleveland, M. Radmacher, D. A. Walters, P. Hillner, M. Bezanilla, M. Fritz, D. Vie, H. G. Hansma, C. B. Prater, J. Massie, L. Fukunaga, J. Gurley, and V. Elings, *Appl. Phys. Lett.* **64**, 1738 (1994).
- [23] S.-T. Yau, D. N. Petsev, B. R. Thomas, and P. G. Vekilov, *J. Mol. Biol.* **303**, 667 (2000).
- [24] N. Ming, K. Tsukamoto, I. Sunagawa, and A. A. Chernov, *J. Cryst. Growth* **91**, 11 (1988).
- [25] L. N. Rashkovich, A. A. Mkrtchyan, and A. A. Chernov, *Sov. Phys. Crystallogr.* **30**, 350 (1985); H. H. Teng, P. M. Dove, C. A. Orme, and J. J. De Yoreo, *Science* **282**, 724 (1998).
- [26] W. K. Burton, N. Cabrera, and F. C. Frank, *Philos. Trans. R. Soc. London A* **243**, 299 (1951).
- [27] J. J. De Yoreo, T. A. Land, and J. D. Lee, *Phys. Rev. Lett.* **78**, 4462 (1997).
- [28] K. Maiwa, M. Plomp, W. J. P. van Enckevort, and P. Bennema, *J. Cryst. Growth* **186**, 214 (1998).
- [29] S.-T. Yau, B. R. Thomas, and P. G. Vekilov, *Phys. Rev. Lett.* **85**, 353 (2000).
- [30] O. Gliko, N. A. Booth, E. Rosenbach, and P. G. Vekilov, *Cryst. Growth Design* **2**, 381 (2002).
- [31] S. Hvidt, *Biophys. Chem.* **39**, 205 (1991).
- [32] M. Pusey, W. Witherow, and R. Naumann, *J. Cryst. Growth* **90**, 105 (1988); H. Lin, F. Rosenberger, J. I. D. Alexander, and A. Nadarajah, *J. Cryst. Growth* **151**, 153 (1995).
- [33] A. A. Chernov, *Modern Crystallography III, Crystal Growth* (Springer-Verlag, Berlin, 1984).
- [34] S. R. Coriell, B. T. Murray, and A. A. Chernov, *J. Cryst. Growth* **149**, 120 (1995).